Journal of Structural Biology **131,** 44–55 (2000)
doi:10.1006/jsbi.2000.4252, available online at http://www.idealibrary.com on IDEAL®

Basement Membrane Macromolecules: Insights from Atomic Force Microscopy

Christine H. Chen and Helen G. Hansma[1]

Department of Physics, University of California, Santa Barbara, California 93106

Received September 27, 1999, and in revised form January 24, 2000

The major macromolecules of basement membranes—collagen IV, laminin-1, and heparan sulfate proteoglycan (HSPG)—have been analyzed by atomic force microscopy (AFM), both individually and in combination with each other. The positions of laminin binding to collagen IV were mapped and compared with the positions of imperfections in the amino acid sequence of collagen IV; the apparent molecular volumes of the HSPG proteoglycans were measured and used to estimate the corresponding molecular weights. Even the thin, thread-like strands of the polyanion heparan sulfate can be visualized with AFM without staining, coating, or fixation. These strands are single polysaccharide chains and are thus thinner than single-stranded DNA. The heparan sulfate strands in HSPG are necessary for protein filtration in kidney basement membranes. We propose that these thin strands filter proteins by functioning as an entropic brush—i.e., that they filter proteins by their constant thermally driven motion in the basement membrane. These AFM analyses in air are a step toward AFM analyses under fluid of basement membrane macromolecules interacting with each other.

Key Words: **atomic force microscopy (AFM); basal lamina; entropic brush; extracellular matrix (ECM); heparan sulfate proteoglycan (HSPG); laminin-1 (Ln-1); molecular volumes; type IV collagen (Col IV); scanning force microscope (SFM); scanning probe microscopy (SPM).**

INTRODUCTION

Good communication between cells is essential for multicellular organisms. Intercellular communication regulates development and differentiation in ways that were once regarded as the exclusive domain of the nucleus. The substructure through which much of this communication occurs is the extracellular matrix. The extracellular matrix is difficult to isolate because it is thin, delicate, and tightly bound to the cells. Although it is difficult to purify intact extracellular matrix, the major macromolecules of the extracellular matrix have been characterized. For the basement membrane, which is a specific type of extracellular matrix, these major macromolecules are laminins, collagen IV, and heparan sulfate proteoglycans.

The explosive growth of this field has been fueled, in part, by the use of recombinant technology for producing basement membrane macromolecules. The wealth of new information in this field is reviewed in alternate years in an entire issue of *Current Opinion Cell Biology* (for editorial overviews, see Ekblom and Timpl, 1996; Horwitz and Thiery, 1994; Horwitz and Werb, 1998). The many other excellent reviews include those of Aumailley and Gayraud (1998); Timpl and Brown (1996); and Yurchenco and O'Rear (1993).

Much of the evidence for the structures of basement membrane macromolecules comes from biochemistry. Direct visualization of these macromolecules (Rohrbach and Timpl, 1993) has been done by electron microscopy, which requires that the molecules be dried, fixed, stained, and imaged in vacuum. Thus atomic force microscopy (AFM) (Binnig *et al.*, 1987; Colton *et al.*, 1997; Hansma and Pietrasanta, 1998; Quate, 1994; Rugar and Hansma, 1990) is a valuable tool for analyzing basement membrane macromolecules in ambient air or in near physiological fluids. As AFM research continues on these vital macromolecules, it will be possible to observe their associations and interactions in near physiological fluids. Intermolecular and intramolecular interactions between and within individual biological molecules are being analyzed not only by AFM imaging but also by pulling on the molecules with the AFM (Florin *et al.*, 1994; Hinterdorfer *et al.*, 1996; Lee *et*

[1] To whom correspondence should be addressed. Fax: (805) 893-8315. E-mail: hhansma@physics.ucsb.edu.

1047-8477/00 $35.00

al., 1994; Moy *et al.*, 1994; Rief *et al.*, 1997). This is another area in which the AFM has a unique ability to unravel secrets of basement membranes.

Previous AFM research on laminin-1 in aqueous fluids illustrates the flexibility of the laminin arms (Chen *et al.*, 1998). Other basement membrane components have not previously been analyzed by AFM. A number of collagens have been analyzed by AFM (Aragno *et al.*, 1995; Chernoff and Chernoff, 1992; Gale *et al.*, 1995; Revenko *et al.*, 1994), but these analyses have not included collagen IV, the collagen that is unique to basement membranes and extracellular matrices.

MATERIALS AND METHODS

Materials

The following macromolecules were stored at −80°C: mouse laminin (Ln-1, 1 mg/ml) and mouse type IV collagen (Col IV, 0.5 mg/ml), both from Gibco-BRL (Grand Island, NY), and heparan sulfate proteoglycan (HSPG, 0.6 mg protein/ml) from Sigma (St. Louis, MO). The laminin may have contained some nidogen/entactin as well, according to the supplier. These macromolecules were purified from the basement membrane of EHS mouse sarcoma tissue.

Buffers

The following buffers were used at pH 7.4: high-salt Mops buffer (20 mM Mops, 5 mM $MgCl_2$, 150 mM NaCl), high-salt Mops buffer with Zn (20 mM Mops, 5 mM $MgCl_2$, 150 mM NaCl, 15 μM $ZnCl_2$), low-salt Mops buffer with Zn (20 mM Mops, 5 mM $MgCl_2$, 25 mM NaCl, 15 μM $ZnCl_2$), and Tris buffer (50 mM Tris, 150 mM NaCl, 5 mM $MgCl_2$).

Sample Preparations for AFM

Disks of mica (Ruby Muscovite mica; New York Mica Co., New York, NY) were glued to steel disks with 2-Ton epoxy (Devcon Corp., Wood Dale, IL) and allowed to dry overnight or longer. The dried mica disks were cleaved with scotch tape immediately before use.

Ln-1 samples (0.01 mg/ml), Col IV samples (0.01–0.02 mg/ml), and HSPG samples (6–60 ng/μl) were prepared with various buffers. Ln-1, Col IV, and HSPG samples were mixed at different concentrations in order to find the best combination/condition suitable for AFM imaging. The mixtures of the samples were allowed to react for 10 min to 2 h. Samples of approximately 1.5 μl were pipetted on to freshly cleaved mica and were left on the mica for approximately 1–5 min. The micas were washed with milliQ water (Millipore Corp., Bedford, MA) and then dried immediately with compressed air. The samples were further dried in a vacuum desiccator over P_2O_5.

AFM Imaging

All data were gathered on a NanoScope III with a Multi Mode AFM (Digital Instruments, Santa Barbara, CA). A vertical-engage E scanner was used, which has maximum scan sizes of 10–15 μm and was calibrated to ca. 8% in the *xy* direction. Scan rates ranged from 6 to 8 Hz, and tapping frequencies ranged from 270 to 330 kHz in air and in dry He gas. All imaging was done with 100-μm silicon cantilevers (Digital Instruments).

Image Analysis

Images were processed by flattening with the NanoScope software. Height Mode images are shown, unless indicated in the text and figure captions. Figures were prepared in Adobe PhotoShop. Gray levels were optimized to display as much of the height information as possible, as in, e.g., Fig. 2C, the relative heights of the collagen strands and the heparan sulfate strand, and in Fig. 4, the relative heights of substructures within individual molecules of laminin and collagen.

Relative molecular volumes of the HSPG protein core were measured with the NanoScope Bearing software in two ways, which gave similar results. The two ways differed in the method for determining the base of the molecule. For some molecules, the Threshold feature of the software was used to visually determine the best area for the base of the molecule. For other molecules, the maximum height of the background was subtracted from the maximum height of the molecule to determine the base of the molecule. Volumes of the molecules were measured from the top of the molecule to the base, as determined by one of these two methods.

RESULTS

Interactions of Collagen IV

Col IV dimers in the AFM typically formed through interactions of the globular NC1 domains, forming linear structures with a globular structure in the center, as in Fig. 1F. These dimers displayed a variety of conformations and interactions, forming loops and folds via different domains (Figs. 1 and 2). Some Col IV dimers folded upon themselves, forming thick overlapped regions (Fig. 1A) or loops (Figs. 1A–1E). Some dimers adhered to other dimers in the triple-helical regions forming lateral associations of supercoils or other superstructures (Figs. 2A and 2B). Intramolecular links were seen, e.g., in Fig. 1A, and intermolecular links in Figs. 1D, 2A, and 2B. Col IV was much easier to image by AFM when it was applied to the substrate in combination with HSPG and/or Ln-1 as opposed to in its pure form. Col IV monomers were measured to be 346 ± 38 nm long.

While the Col IV interactions in Figs. 1 and 2 can be seen via obvious domain interactions, the Col IV interactions in Fig. 3 were more subtle. Here the points of interactions between individual molecules are less obvious, since there are no thick overlapping regions or well-defined globular domains on the polymer.

Laminin Binding to Collagen IV

Ln-1 binding to Col IV was observed on the globular NC1 domain of Col IV and at several positions on the Col IV triple helix (Fig. 4). The three most frequent binding sites on the triple helical region were at the following distances from the globular NC1 domain: 70 ± 10 nm (19% of molecules), 180 ± 20 nm (27% of molecules), and 300 ± 20 nm (32% of molecules) (Fig. 4G). Ln-1 binding to Col IV was also observed at the globular NC1 domain (14% of molecules) and at ~240 nm (8% of molecules).

Ln-1 and Col IV were applied to the mica surface in buffers with or without Zn(II). Zn(II) promotes the

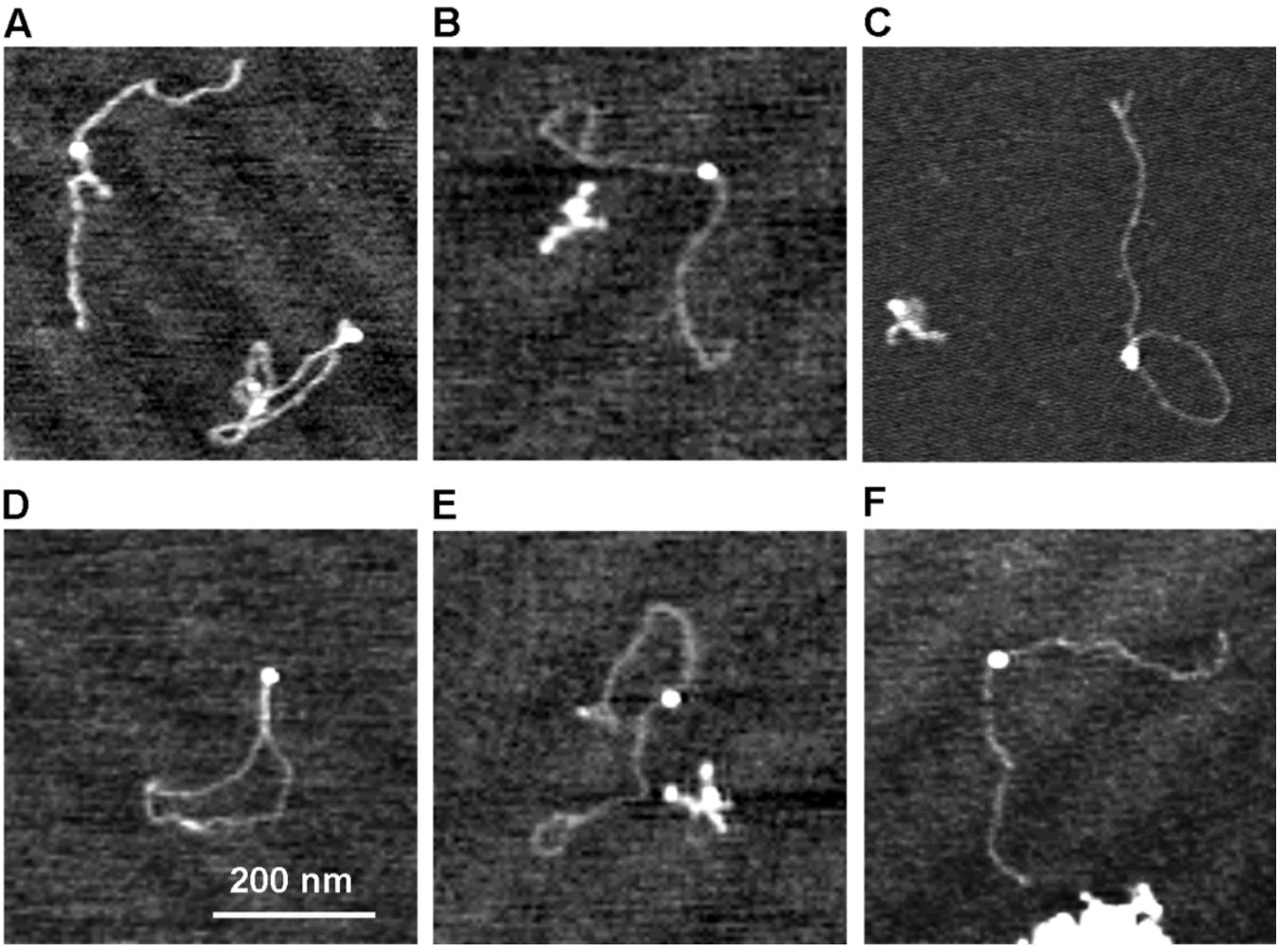

FIG. 1. Collagen IV dimers and their intramolecular interactions. Laminin molecules can also be seen in B, C, and E and in a clump in F. Reaction mixtures containing 10 ng/μl Ln-1 + 10–20 ng/μl Col IV were incubated 1 h in a test tube: (A, B, and D–F) in Mops buffer; (C) in Mops buffer + Zn(II); image sizes, 500 × 500 nm.

binding of Ln-1 to Col IV, as measured by an enzyme-linked immunosorbent assay (Ancsin and Kisilevsky, 1996). Zn(II) also promotes binding of DNA to mica for AFM imaging in fluid (Hansma and Laney, 1996). Our AFM analyses showed interactions between Ln-1 and Col IV in both the presence and the absence of Zn(II); we did not quantitate these analyses to determine whether Zn(II) increased the binding of Ln-1 to Col IV as observed by AFM.

Heparan Sulfate Proteoglycans

The heparan sulfate chains of HSPG are visualized by AFM as very thin threads (Fig. 2C, white arrow). Individual HSPG molecules were not well resolved in samples containing only HSPG. In dilute samples, HSPG did not bind well to mica, since the negative charges of the heparan sulfate chains did not bind to the negatively charged mica. Concentrated samples had another problem—aggregation (Fig. 5). Any individual molecules of HSPG were obscured by the aggregates.

A phase image of HSPG aggregates shows prominent light patches that are barely visible in the height image (Fig. 5B). These light patches appeared in some phase images of HSPG molecules alone but not in phase images of HSPG molecules incubated with Ln-1 or Col IV.

Many individual HSPG molecules were observed in the samples of HSPG mixed with Col IV and Ln-1 (Fig. 6). Ln-1, in particular, seems to disrupt the aggregates of HSPG.

The individual HSPG molecules had ~3–4 thread-like chains attached to a beaded globular core (Fig. 6). The conformations of the heparan sulfate chains were variable and included chains that

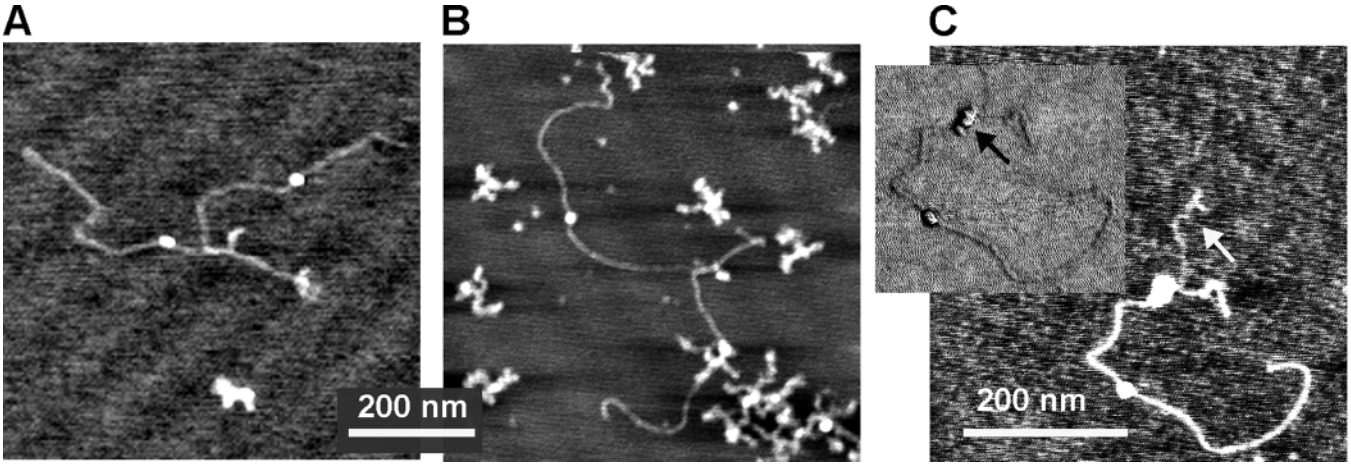

FIG. 2. Collagen IV intermolecular interactions. (A and B) Interactions between pairs of collagen IV dimers. One laminin molecule can also be seen in (A) and many in (B). Reaction conditions are same as those Fig. 1A. (C) Collagen IV dimer with HSPG; 10 ng/μl each, Ln-1 + Col IV; 6 ng/μl HSPG in low-salt Mops with Zn. Phase image (inset) shows beaded structure of proteoglycan core of HSPG (black arrow). White arrow shows heparan sulfate chain of HSPG; image sizes: (A, B) 665 × 665 nm; (C) 500 × 500 nm.

were stretched out, aggregated to each other, or adhered to the protein core. The protein core was elongated and bead-like in most of the HSPG molecules (Figs. 6A, 6D, and 7E); the protein core was small or semicircular in a few HSPG molecules.

The tails of most HSPG molecules project out from only one end of the protein core (Figs. 6A, 6B, right molecule, 6C, left molecule, 6D, and 7D), but a few seem to project from all around the protein core (Fig. 6F, upper molecule; Fig. 7C). The HSPG in Fig. 6E appears to have fragmented, resulting in the separation of heparan sulfate chains from a protein core.

The molecular volumes of the HSPG protein cores measured by AFM (Fig. 6) are 290 ± 100 nm^3 for the smaller protein cores and 710 ± 90 nm^3 for the larger protein cores. For comparison, the measured volumes are 320 ± 80 nm^3 for dimers of the Col IV NC1 domain, 1000 ± 160 nm^3 for Ln-1 and 2100 ± 230 nm^3 for dimers of Ln-1.

HSPG Interacting with Laminin and Col IV

Our images showed HSPG interacting primarily with Ln-1 (Fig. 7) and occasionally with Col IV (Fig. 2C).

Interactions between HSPG molecules and Ln-1 molecules were often observed (Fig. 7). Most of the HSPG molecules were attached to Ln-1's long arms via their heparan sulfate chains (Figs. 7B–7E).

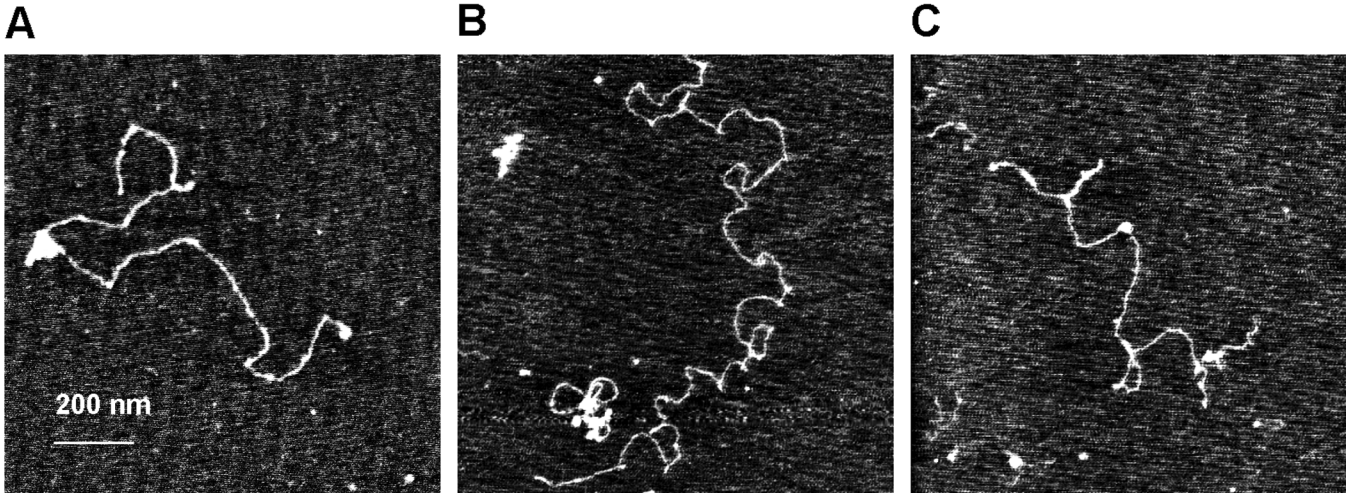

FIG. 3. Collagen IV multimers. Reaction mixture containing Col IV, Ln-1, and HSPG. For reaction mixture, see Fig. 2C. Laminin molecules can also be seen on the left sides of (A) and (B), and HSPG can be seen in the lower right corner of (C); image sizes, 1000 × 1000 nm.

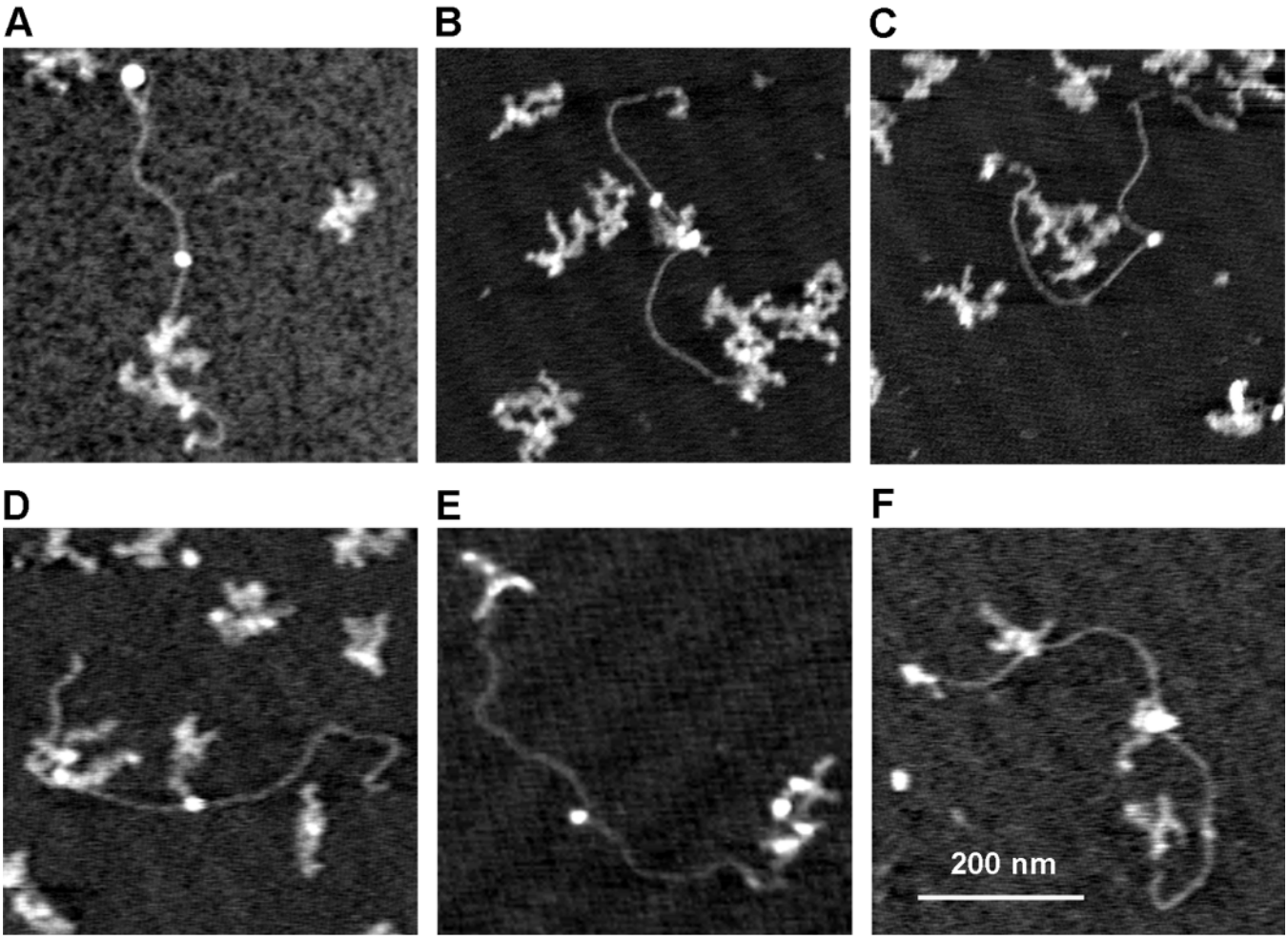

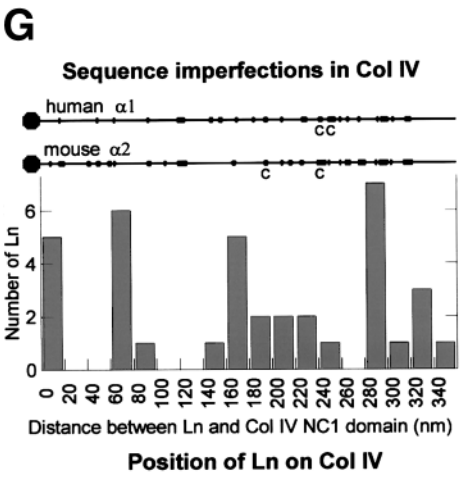

FIG. 4. Interactions of laminin with collagen IV (A–G) and sequence imperfections in Col IV polypeptide chains (G). (A–F) Laminin bound to collagen IV dimers. For reaction mixture, see Fig. 1A; image sizes, 500 × 500 nm. (G) Histogram of the positions of Ln-1 on Col IV, measured from the globular C-terminal NC1 domain of Col IV. The number at the bottom of each bar is the lower value for the bin represented by that bar; e.g., the first bar on the left represents the range 0–19 nm. Diagram at the top of G maps the locations of imperfections, i.e., replacements of Gly in the Gly-X_{aa}-Y_{aa} repeating sequence, of human α1 and mouse α2 triple-helical regions of the Col IV polypeptides. Lengths of bars in the Col IV diagram are 5–10 times longer than the actual relative lengths of the imperfections in the Col IV sequence. The C's mark regions containing one or two cysteine residues. Black balls show the locations of the NC1 domains. The diagram was adapted from Yamada and Kuehn (1993).

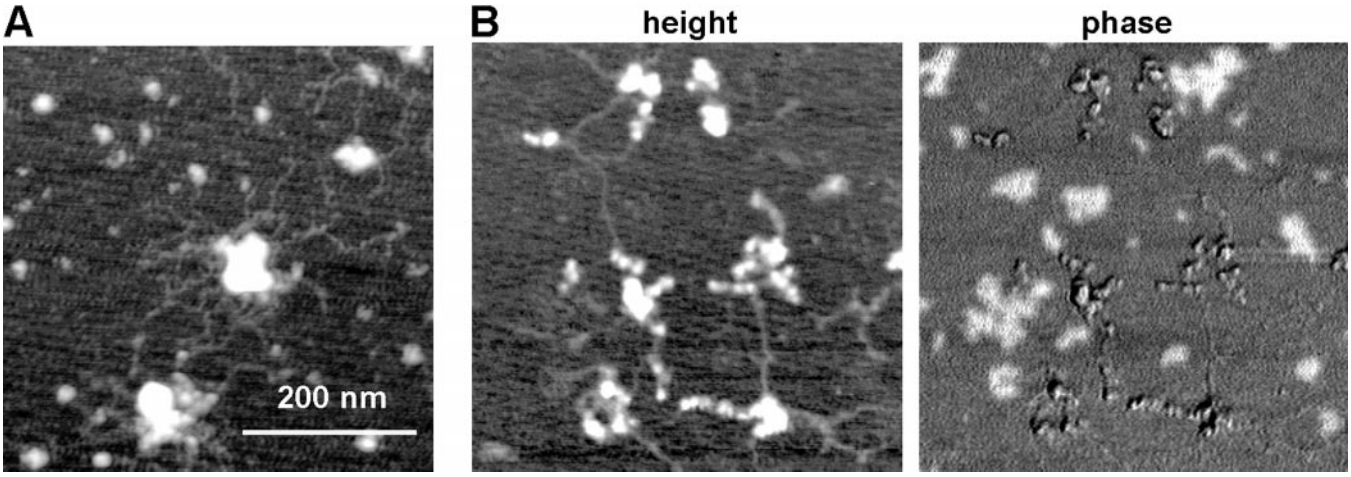

FIG. 5. HSPG aggregates. (A) Height image; (B) simultaneously acquired height and phase images of the same area. Reaction mixtures: (A) 60 ng/μl HSPG + 5 ng/μl Col IV in Mops buffer with Zn; (B) 60 ng/μl HSPG in Tris buffer; image sizes, 500 × 500 nm.

Some heparan sulfate chains of a single HSPG molecule seem to bind to more than one Ln-1 molecule (Fig. 7).

DISCUSSION

The substructures and interactions of Ln-1, Col IV, and HSPG were analyzed by AFM in air. AFM in aqueous fluid has failed thus far to resolve basement membrane components other than Ln-1 (Chen *et al.*, 1998). This important accomplishment will require further research.

AFM analyses of new biomaterials typically require the development of new methods for sample preparation. In the present work, we developed successful methods for imaging basement membrane macromolecules in air. It is, however, much more difficult to develop methods for analyzing biological macromolecules under aqueous fluid, which tends to dissolve the biomolecules.

Collagen IV and Its Interactions

Col IV are usually the major structural component of basement membranes, although laminin and HSPG alone form a morphologically normal-appearing basement membrane in a tumor cell line that lacks Col IV (Noonan and Hassell, 1993).

Col IV molecules have a triple-helical region, ~1400 amino acids long (Hudson, 1993), whose length is 355 nm long by EM (Timpl, 1981) and 346 ± 38 nm long by AFM. The globular C-terminal domains of Col IV molecules dimerize (Yurchenco and O'Rear, 1993) to form the structures seen in Figs. 1, 2, and 4. Figure 1F is an especially clear image of a Col IV dimer.

The Col IV dimer in Fig. 1D shows an interaction at the N-terminal domain, where there is a short thick region at the bottom of the loop, indicating an overlap of ~20 nm between the two N-terminal domains. This is the first step in the aggregation of four Col IV molecules at their N-termini (Yamada and Kuehn, 1993). The triple-helical N-termini of two Col IV molecules overlap in an anti-parallel direction along their first 117 amino acid residues. They bind through hydrophobic interactions and then bond covalently through intermolecular disulfide bridges and lysine links. Pairs of these dimers overlap to form a tetramer, which can be isolated by proteolysis as a fragment with a sedimentation coefficient of 7S (Yurchenco and O'Rear, 1993).

Col IV molecules are heterotrimers with three polypeptide chains [α1(IV)$_2$$\alpha$2(IV)], which combine to form the C-terminal globular domain (NC1) and a long triple-helical domain, terminating in the N-terminal 7S domain (Timpl and Brown, 1996; Yurchenco and O'Rear, 1994). Through these domains, Col IV molecules interact to form networks with each other or with other components of basement membranes. The lateral associations from these intermolecular links are believed to be a major source of the fine branching structures seen in basement membrane networks. Because many binding options are possible, i.e., end-to-end, helix-to-helix, and helix-to-end (Yurchenco and O'Rear, 1994), Col IV may play a significant role in contributing diversity to the architecture and mechanical stability of basement membrane networks.

Col IV triple helices are more flexible than the triple helices of fibrillar collagens. This flexibility is evident in Figs. 1 and 2, where the longest straight region of the collagen molecules is ~100 nm. The polypeptide chains in the triple helices of Col IV have many "imperfections," or interruptions of the

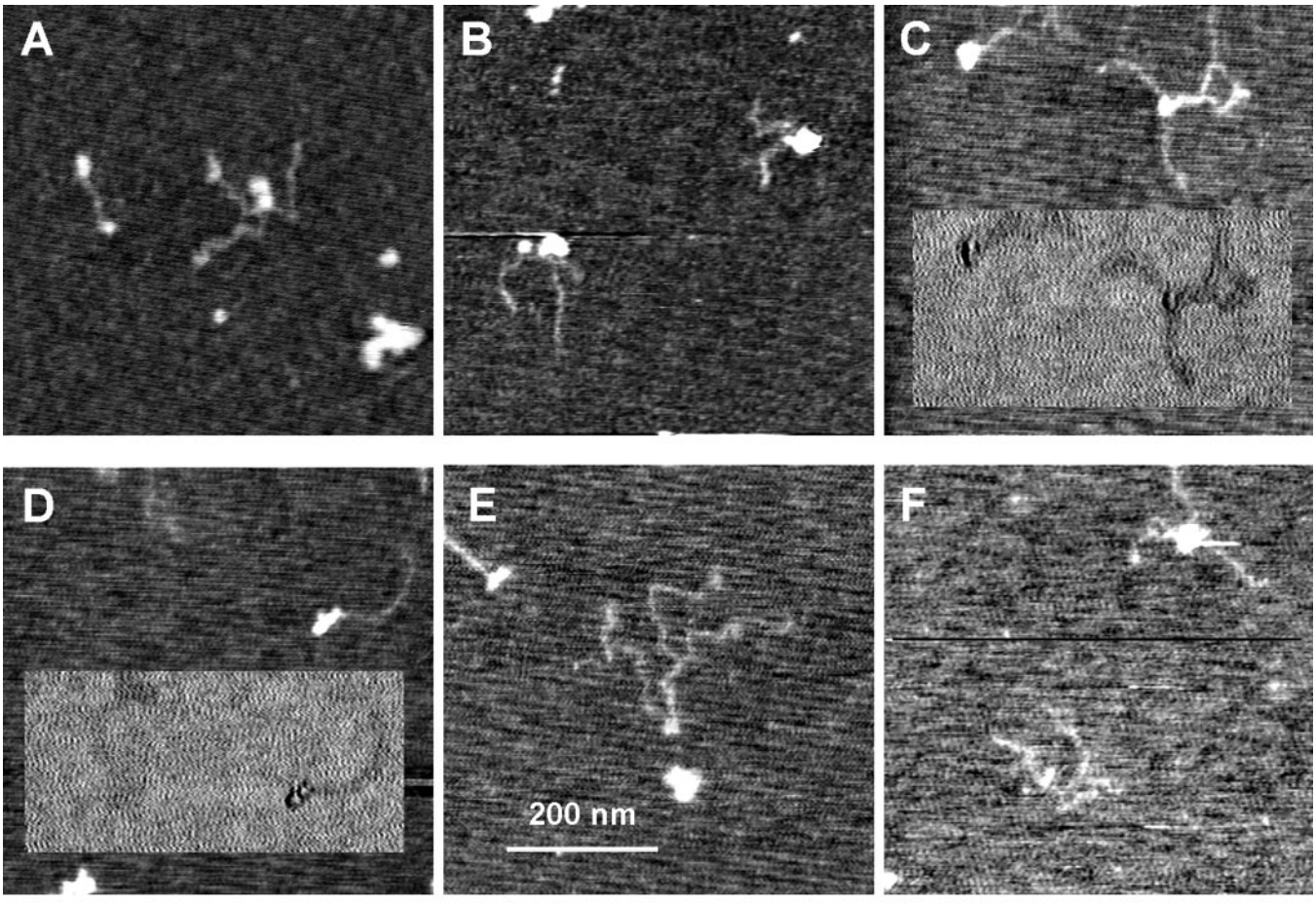

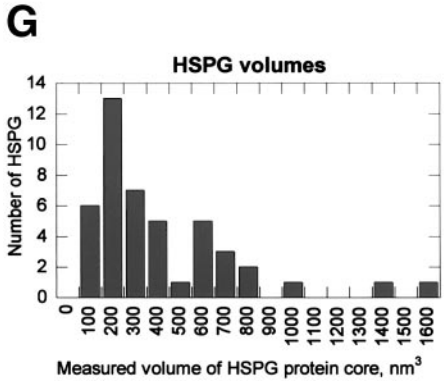

FIG. 6. (A–F) HSPG molecules seen in reaction mixtures containing HSPG + Ln-1 + Col IV. Reaction mixtures contained 10 ng/μl each Ln-1 + Col IV and 6–10 ng/μl HSPG in low-salt Mops buffer with Zn. Insets are phase images; image sizes, 500 × 500 nm. (F) The two HSPG molecules in this image were cropped from a larger image, where they were actually separated by a larger distance on the mica surface, as indicated by the black line. (G) Histogram of the measured volumes of the protein core of HSPG molecules. Measured volumes include the contribution of the tip to the volume and are therefore relative volumes and not actual volumes of the HSPG protein cores. The number at the bottoms of each bar is the lower value for the bin represented by that bar; e.g., the first bar on the left represents the range 0–99 nm^3.

Gly-X_{aa}-Y_{aa} amino acid sequence that forms stable alpha helices (Hudson, 1993). The diagram at the top of Fig. 4G shows the locations of these imperfections an α1 and an α2 Col IV polypeptide chain (Yamada and Kuehn, 1993; see also Blumberg *et al.*, 1988; Hostikka and Tryggvason, 1988; Hudson, 1993; Pettitt and Kingston, 1991; Saus *et al.*, 1989). In contrast to Col IV, the triple helical domains

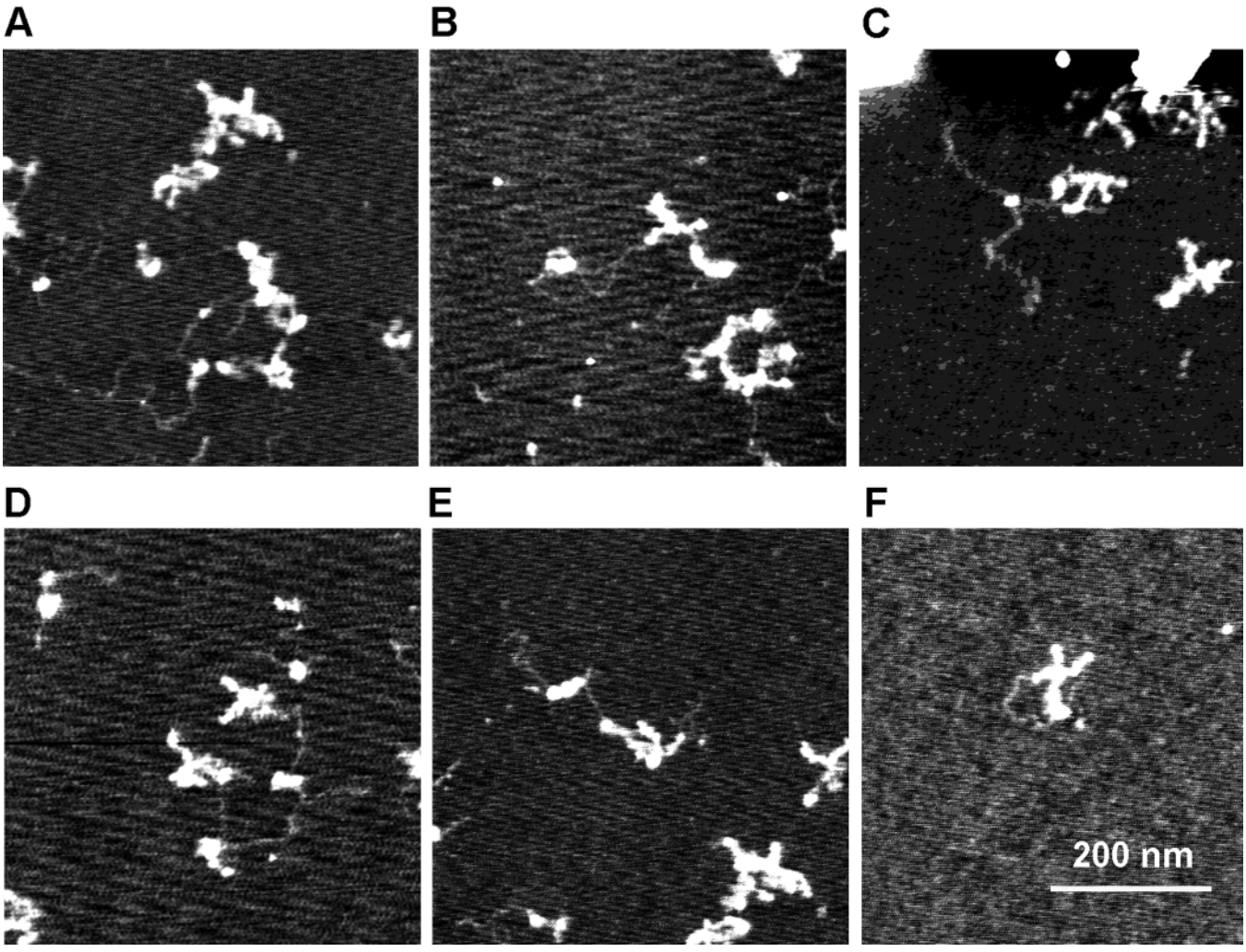

FIG. 7. Interactions of HSPG and Ln-1. For some images, reaction mixtures are the same as those for Fig. 2C; for other images, reaction mixtures contain high-salt Mops buffer with Zn(II), 10 ng/μl Ln-1 + 6 ng/μl HSPG; image sizes, 500 × 500 nm.

of fibrillar collagens generally have uninterrupted sequences of Gly-X_{aa}-Y_{aa} and form stable alpha helices.

Laminin Binding to Collagen IV

Ln-1 molecules have a distinctive cruciform structure with globular domains in the arms of the cross, as seen by TEM and sequence analyses (Timpl and Brown, 1994) and by AFM in air (Chen *et al.*, 1998). Time-lapse AFM in near physiological fluids also reveals considerable flexibility in the four arms of Ln-1 (Chen *et al.*, 1998).

The binding of Ln-1 to Col IV has been mapped by AFM (Fig. 4G) and TEM. The maps are similar. With TEM, Ln-1 binding was observed everywhere along Col IV except in a region ~120–150 nm from the globular NC1 domain; binding maxima were at ~81, 216, and 295 nm away from the NC1 domain (Laurie, 1986).

Recent sequence analyses of Col IV allow a comparison mapping of Col IV sequence imperfections with Ln-1 binding (Fig. 4G). Both Col IV sequence imperfections and Ln-1 binding are distributed widely along the Col IV triple-helical region. The sequence imperfections and Ln-1 binding are both more pronounced along the half of the Col IV triple helix that is distant from the NC1 domain. More precisely, two thirds of the Ln-1 binding in Fig. 4G and two thirds of the sequence imperfections occur on the distal or N-terminal half of the Col IV triple helix. There is a surprisingly constant 2:1 ratio of proximal-to-distal imperfections seen in both α1 and α2 Col IV chains from five different animal species, based on the diagrams in Yamada and Kuehn

(1993). These results suggest that Ln-1 binds preferentially to sequence imperfections.

The data are not yet sufficient, however, to prove that Ln-1 binds to sequence imperfections. In Fig. 4G, the actual positions of Ln-1 binding correspond only weakly with the positions of sequence imperfections. This indicates that there are flaws, either the hypothesis or in the quantity and quality of the Ln-1 binding data. The problem with data quality is illustrated by two different plots of the same data for laminin binding to Col IV, in which the position of laminin on Col IV is plotted vs either the fractional distance along Col IV or the distance in nm from the NC1 domain of Col IV (Laurie, 1986). The plot of laminin binding vs distance in nm from the NC1 domain looks similar to that of Fig. 4G, while the plot of laminin binding vs fractional distance along Col IV looks quite different, with maximal binding seen at a position 20% of the distance from the NC1 domain.

Another study of Ln-Col IV binding raises questions about the hypothesis that Ln-1 binds to Col IV sequence imperfections (Charonis *et al.*, 1986). In this study, Ln-1 binding to Col IV was mapped in the presence of one or the other of two different antibodies. In the presence of a nonspecific antibody, anti-BSA, two thirds of the Ln-1 binding occurred in the half of the Col IV triple helix that is proximal to the NC1 domain, and this proximal binding was primarily located at a position ~30% of the distance from the NC1 domain. In the presence of a specific antibody to the E3 fragment of Ln-1, the binding of Ln-1 to Col IV was significantly reduced and randomly distributed.

Heparan Sulfate Proteoglycans

HSPG molecules have beaded globular protein cores with thread-like heparan sulfate chains projecting from them (Paulsson *et al.*, 1987). Heparan sulfate is a single polysaccharide chain, which makes it thinner than the Col IV triple helix and thinner than nucleic acids such as double-stranded or single-stranded DNA, which have been imaged by AFM (Hansma *et al.*, 1996). The contrast in height between heparan sulfate and triple-helical Col IV is especially dramatic when one compares the appearance of the Col IV triple helix in Fig. 2C with the Col IV triple helixes in Figs. 2A and 2B.

Molecular volumes measured from AFM images often give a reliable estimate of the molecular weight of the biomolecules being imaged (Golan *et al.*, 1999; Pietrasanta *et al.*, 1999; Schneider *et al.*, 1998). When molecular volumes are measured for macromolecules of known molecular weights, the calculated densities of these macromolecules typically fall in the range of 1–1.5 g/ml. This is within the expected density range for macromolecules such as proteins. With Ln-1, for example, the measured volume of 1000 nm^3 and the molecular weight of 820 kDa (Timpl and Brown, 1994) give a density of 1.4 g/ml. Using this density to estimate molecular weights for HSPG gives 240 and 600 kDa, respectively, for the small and large proteoglycan cores of HSPG.

Basement membranes contain a variety of HSPG molecules including perlecan and agrin (Timpl, 1996). Perlecan has a proteoglycan core of ~400–500 kDa, with two to three heparan sulfate side chains issuing from one end of the protein core (Iozzo *et al.*, 1994). Agrin has a smaller proteoglycan core of ~250 kDa (Tsen *et al.*, 1995). The proposed structure of the perlecan protein core, from cDNA and other analyses, is a string of globules resembling various known protein domains and a unique sequence at the N-terminus, where the heparan sulfate chains are attached. The known protein domains found in perlecan are related to the LDL receptor, various laminin domains, and repeats of the immunoglobulin-like N-CAM sequence (Noonan and Hassell, 1993).

HSPG tended to aggregate when applied to mica in the absence of Ln-1 or Col IV (Fig. 5). HSPG also exhibit a high tendency for aggregation in solution, as measured by sedimentation velocity centrifugation or electron microscopy (Paulsson *et al.*, 1987).

Some phase AFM images of HSPG aggregates had light patches (Fig. 5B). These light patches in the phase images mapped at locations on the height images that sometimes showed no features at all and were always less than 0.2 nm higher than the mica surface. We have not been able to identify these patches, which do not appear to be residual buffer, since such patches were not seen in images of buffer alone. Light patches in phase images tend to correspond to regions in the image where there is reduced adhesion between the tip and the sample (Argaman *et al.*, 1997). Mica, which is generally more adhesive than biomolecules (Hansma, 1996; Radmacher *et al.*, 1994), is darker in these phase images. Phase images in tapping AFM show the phase difference between the oscillation driving the cantilever and the oscillation of the cantilever as it interacts with the sample surface (Babcock and Prater, 1995). In air, phase images are a measure of the energy dissipated by the tip–sample interaction (Cleveland *et al.*, 1998). The degree of adhesion between the tip and the sample correlates with the darkness in the phase image, if the tip is imaging at a force high enough to produce a repulsive interaction with the surface.

Thus, phase imaging, as in Fig. 5B, can sometimes detect properties of the sample surface that are not

readily detected in height images. Phase images also showed more clearly the beaded structures of the HSPG protein cores (Figs. 2C, inset, 5B, and 6, insets).

HSPG Interacting with Laminin and Col IV

Our images showed HSPG interacting primarily with Ln-1 (Fig. 7) and occasionally with Col IV (Fig. 2C). In Fig. 2C, the beaded protein core of HSPG interacts with the Col IV triple helix. This contrasts with results from affinity chromatography that showed HSPG interacting with Col IV and Ln-1 only via its heparan sulfate chains (Fujiwara, 1984; Sakashita, 1980; Woodley, 1983).

Entropic Brushes

HSPG are highly charged due to their anionic heparan sulfate strands. These heparan sulfate strands provide a selective filtration barrier in basement membranes, such as those of kidney glomeruli (Kasinath and Kanwar, 1993). The selective filtration barrier in kidney basement membranes prevents blood proteins from entering the urine. When heparan sulfate is removed from kidney basement membranes with the enzyme heparitinase, albumin passes readily from the blood into the urine (Kasinath and Kanwar, 1993; Noonan and Hassell, 1993).

One hypothesis for the way in which the heparan sulfate strands of HSPG can block the flow of proteins from the blood to the urine is that the tiny strands of heparan sulfate act as an entropic brush (Hoh, 1998; Milner, 1991). An entropic brush is a confined polymer in constant thermally driven motion. The heparan sulfate polymers of HSPG are confined by being tethered to the protein core of HSPG. The heparan sulfate strands extend away from the protein core of HSPG because of the electrostatic repulsion between the anionic sulfates. The thermal motion of these extended chains of HSPG can impede the flow of proteins across the basement membrane without impeding the flow of small molecules. In this way HSPG can provide a barrier to the flow of proteins without distorting the information-rich connections between laminin and its receptor, integrin, on the cell membrane.

Another emerging theme in basement membrane research is the role of proteases, which can activate adhesion (Horwitz and Werb, 1998). It has been hypothesized that activation/inactivation by proteases is due to the proteolytic removal of entropic brushes or entropic bristle domains (Hoh, 1998). Entropic brushes and entropic bristle domains are mobile and disordered; therefore they repel molecules or surfaces that come close enough to confine them and reduce their entropy.

Thus protease-activated adhesion in basement membranes may be due to the proteolytic removal of entropic bristle domains. The removal of these disordered entropic bristle domains would permit the stable intermolecular interactions required for adhesion.

Conclusion

New examples are constantly arising for the biomedical importance of research on basement membranes. Major problems in basement membranes have long been observed among patients with diabetes and other kidney diseases (Rohrbach and Murrah, 1993; Tryggvason *et al.*, 1993). The number of known basement membrane diseases is growing (Krieg and LeRoy, 1998). More recently, basement membranes and the extracellular matrix are suspects in the many problems of connective tissues that develop with aging (Robert, 1998). Tissue engineering is another area where basement membrane research is contributing directly to the development of techniques for regenerating tissues and organs as an alternative to organ transplant (Kim and Mooney, 1998). These examples illustrate the benefits of understanding the functions of basement membrane components and how they interact with one another to organize a functional basement membrane matrix. The research presented here is a beginning toward using the AFM as a tool for some of this vital research into basement membranes.

We thank Dennis Clegg and Jan Hoh for helpful discussions, Paul Hansma and Dan Morse for their generous assistance in support of this research, Lia Pietrasanta, Tilman Schaffer, and Roxana Golan for valuable technical assistance, and Scott Hansma for developing NanoConvert, a tiff conversion software for NanoScope images. This work was supported by NSF MCB 9604566 (H.H.), Digital Instruments, and the U. S. Army Research Office Multidisciplinary University Research Initiative DAAH04-96-1-0443 (C.C.).

REFERENCES

Ancsin, J. B., and Kisilevsky, R. (1996) Laminin interactions important for basement membrane assembly are promoted by zinc and implicate laminin zinc finger-like sequences, *J. Biol. Chem.* **271,** 6845–6851.

Aragno, I., Odetti, P., Altamura, F., Cavalleri, O., and Rolandi, R. (1995) Structure of rat tail tendon collagen examined by atomic force microscope, *Experientia* **51,** 1063–1067.

Argaman, M., Golan, R., Thomson, N. H., and Hansma, H. G. (1997) Phase imaging of moving DNA molecules and DNA molecules replicated in the atomic force microscope, *Nucleic Acids Res.* **25,** 4379–4384.

Aumailley, M., and Gayraud, B. (1998) Structure and biological activity of the extracellular matrix, *J. Mol. Med.* **76,** 253–265.

Babcock, K. L., and Prater, C. B. (1995) Phase Imaging: Beyond Topography, Digital Instruments, Santa Barbara, CA.

Binnig, G., Gerber, C., Stoll, E., Albrecht, R. T., and Quate, C. F.

(1987) Atomic resolution with atomic force microscope, *Europhys. Lett.* **3,** 1281–1286.

Blumberg, B., MacKrell, A. J., and Fessler, J. H. (1988) Drosophila basement membrane procollagen alpha 1(IV). II. Complete cDNA sequence, genomic structure, and general implications for supramolecular assemblies, *J. Biol. Chem.* **263,** 18328–18337.

Charonis, A. S., Tsilibary, E. C., Saku, T., and Furthmayr, H. (1986) Inhibition of laminin self-assembly and interaction with type IV collagen by antibodies to the terminal domain of the long arm, *J. Cell Biol.* **103,** 1689–1697.

Chen, C. H., Clegg, D. O., and Hansma, H. G. (1998) Structures and dynamic motion of laminin-1 as observed by atomic force microscopy, *Biochemistry* **37,** 8262–8267.

Chernoff, E. A. G., and Chernoff, D. A. (1992) Atomic force microscope images of collagen fibers, *J. Vac. Sci. Technol. A* **10,** 596–599.

Cleveland, J. P., Anczykowski, B., Schmid, A. E., and Elings, V. B. (1998) Energy dissipation with a tapping-mode atomic force microscope, *Appl. Phys. Lett.* **72,** 2613–2615.

Colton, R. J., Baselt, D. R., Dufrene, Y. F., Green, J. B. D., and Lee, G. U. (1997) Scanning probe microscopy, *Curr. Opin. Chem. Biol.* **1,** 370–377.

Ekblom, P., and Timpl, R. (1996) A multifaceted aproach emerging, *Curr. Opin. Cell Biol.* **8,** 599–601.

Florin, E.-L., Moy, V. T., and Gaub, H. E. (1994) Adhesion forces between individual ligand-receptor pairs, *Science* **264,** 415–417.

Fujiwara, S., Wiedemannn, H., Timpl, R., Lustig, A., and Engel, J. (1984) Structure and interactions of heparan sulfate proteoglycans from a mouse tumor basement membrane, *Eur. J. Biochem.* **143,** 145–157.

Gale, M., Pollanen, M. S., Markiewicz, P., and Goh, M. C. (1995) Sequential assembly of collagen revealed by atomic force microscopy, *Biophys. J.* **68,** 2124–2128.

Golan, R., Pietrasanta, L. I., Hsieh, W., and Hansma, H. G. (1999) DNA toroids: Stages in condensation, *Biochemistry* **38,** 14069–14076.

Hansma, H. G. (1996) Atomic force microscopy of biomolecules, *J. Vac. Sci. Technol. B* **14,** 1390–1394.

Hansma, H. G., and Laney, D. E. (1996) DNA binding to mica correlates with cationic radius: Assay by atomic force microscopy, *Biophys. J.* **70,** 1933–1939.

Hansma, H. G., and Pietrasanta, L. (1998) Atomic force microscopy and other scanning probe microscopies, *Curr. Opin. Chem. Biol.* **2,** 579–584.

Hansma, H. G., Revenko, I., Kim, K., and Laney, D. E. (1996) Atomic force microscopy of long and short double-stranded, single-stranded and triple-stranded nucleic acids, *Nucleic Acids Res.* **24,** 713–720.

Hinterdorfer, P., Baumgartner, W., Gruber, H. J., Schilcher, K., and Schindler, H. (1996) Detection and localization of individual antibody-antigen recognition events by atomic force microscopy, *Proc. Natl. Acad. Sci. USA* **93,** 3477–3481.

Hoh, J. H. (1998) Functional protein domains from the thermally driven motion of polypeptide chains: A proposal, *Proteins—Struct. Funct. Genet.* **32,** 223–228.

Horwitz, A. F., and Thiery, J. P. (1994) Cell-to-cell contact and extracellular matrix, *Curr. Opin. Cell Biol.* **6,** 645–647.

Horwitz, A. R., and Werb, Z. (1998) Cell adhesion and the extracellular matrix: Recent progress and emerging themes, *Curr. Opin. Cell Biol.* **10,** 563–565.

Hostikka, S. L., and Tryggvason, K. (1988) The complete primary structure of the alpha 2 chain of human type IV collagen and comparison with the alpha 1(IV) chain, *J. Biol. Chem.* **263,** 19488–19493.

Hudson, B. G., Reeders, S. T., and Tryggvason, K. (1993) Type IV Collagens: Structure, gene organization, and role in human diseases, *J. Biol. Chem.* **268,** 26033–26036.

Iozzo, R. V., Cohen, I. R., Grässel, S., and Murdoch, A. D. (1994) The biology of perlecan: The multifaceted heparan sulphate proteoglycan of basement membranes and pericellular matrices, *Biochem. J.* **302,** 625–639.

Kasinath, B. S., and Kanwar, Y. S. (1993) Glomerular basement membrane: Biology and physiology, *in* D. H. Rohrbach and R. Timpl (Eds.), Molecular and Cellular Aspects of Basement Membranes, Academic Press, New York.

Kim, B. S., and Mooney, D. J. (1998) Development of biocompatible synthetic extracellular matrices for tissue engineering, *Trends Biotechnol.* **16,** 224–230.

Krieg, T., and LeRoy, E. C. (1998) Diseases of the extracellular matrix [editorial], *J. Mol. Med.* **76,** 224–225.

Laurie, G. W., Bing, J. T., Kleinman, H. K., Hassell, J. R., Aumailley, M., Martin, G. R., and Feldmann, R. J. (1986) Localization of binding sites for laminin, heparan sulfate proteoglycan and fibronectin on basement membrane (Type IV) collagen, *J. Mol. Biol.* **189,** 205–216.

Lee, G. U., Chrisey, L. A., and Coulton, R. J. (1994) Direct measurement of the forces between complementary strands of DNA, *Science* **266,** 771–773.

Milner, S. T. (1991) Polymer brushes, *Science* **251,** 905–914.

Moy, V. T., Florin, E.-L., and Gaub, H. E. (1994) Intermolecular forces and energies between ligands and receptors, *Science* **266,** 257–259.

Noonan, D. M., and Hassell, J. R. (1993) Proteoglycans of basement membranes, *in* D. H. Rohrbach and R. Timpl (Eds.), Molecular and Cellular Aspects of Basement Membranes, pp. 189–210, Academic Press, San Diego.

Paulsson, M., Yurchenco, P. D., Ruben, G. C., Engel, J., and Timpl, R. (1987) Structure of low density heparan sulfate proteoglycan isolated from a mouse tumor basement membrane, *J. Mol. Biol.* **197,** 297–313.

Pettitt, J., and Kingston, I. B. (1991) The complete primary structure of a nematode alpha 2(IV) collagen and the partial structural organization of its gene, *J. Biol. Chem.* **266,** 16149–16156.

Pietrasanta, L. I., Thrower, D., Hsieh, W., Rao, S., Stemmann, O., Lechner, J., Carbon, J., and Hansma, H. G. (1999) Probing the *Sacchromyces cervisiae* CBF3-*CEN* DNA kinetochore complex using atomic force microscopy, *Proc. Natl. Acad. Sci. USA* **96,** 3757–3762.

Quate, C. F. (1994) The AFM as a tool for surface imaging, *Surface Sci.* **299/300,** 980–995.

Radmacher, M., Cleveland, J. P., Fritz, M., Hansma, H. G., and Hansma, P. K. (1994) Mapping interaction forces with the atomic force microscope, *Biophys. J.* **66,** 2159–2165.

Revenko, I., Sommer, F., Minh, D. T., Garrone, R., and Franc, J. M. (1994) Atomic force microscopy study of the collagen fibre structure, *Biol. Cell* **80,** 67–69.

Rief, M., Gautel, M., Oesterhelt, F., Fernandez, J. M., and Gaub, H. E. (1997) Reversible unfolding of individual titin immunoglobulin domains by AFM, *Science* **276,** 1109–1112.

Robert, L. (1998) Mechanisms of aging of the extracellular matrix: Role of the elastin-laminin receptor, *Gerontology* **44,** 307–317.

Rohrbach, D. H., and Murrah, V. A. (1993) Molecular aspects of basement membrane pathology, *in* D. H. Rohrbach and R.

Timpl (Eds.), Molecular and Cellular Aspects of Basement Membranes, pp. 386–420, Academic Press, San Diego, CA.

Rohrbach, D. H., and Timpl, R. (1993) Molecular and Cellular Aspects of Basement Membranes, Academic Press, New York.

Rugar, D., and Hansma, P. K. (1990) Atomic force microscopy, *Phys. Today* **43,** 23–30.

Sakashita, S., Engvall, E., and Ruoslahti, E. (1980) Basement membrane glycoprotein laminin binds to heparin, *FEBS Lett.* **116,** 243–246.

Saus, J., Quinones, S., MacKrell, A., Blumberg, B., Muthukumaran, G., Pihlajaniemi, T., and Kurkinen, M. (1989) The complete primary structure of mouse alpha 2(IV) collagen: Alignment with mouse alpha 1(IV) collagen, *J. Biol. Chem.* **264,** 6318–6324.

Schneider, S. W., Larmer, J., Henderson, R. M., and Oberleithner, H. (1998) Molecular weights of individual proteins correlate with molecular volumes measured by atomic force microscopy, *Pflugers Arch.* **435,** 362–367.

Timpl, R., Wiedemann, H., Delden, V. V., Furthmayr, H., and Kuhn, K. (1981) A network model for the organization of type IV collagen molecules in basement membranes, *Eur. J. Biochem.* **120,** 203–211.

Timpl, R. (1996) Macromolecular organization of basement membranes, *Curr. Opin. Cell Biol.* **8,** 618–624.

Timpl, R., and Brown, J. (1994) The laminins, *Matrix Biol.* **14,** 275–281.

Timpl, R., and Brown, J. C. (1996) Supramolecular assembly of basement membranes, *Bioessays* **18,** 123–132.

Tryggvason, K., Zhou, J., and Hostikka, S. L. (1993) Alport syndrome and other inherited basement membrane disorders, *in* D. H. Rohrbach and R. Timpl (Eds.), Molecular and Cellular Aspects of Basement Membranes, pp. 421–438, Academic Press, San Diego, CA.

Tsen, G., Halfter, W., Kroeger, S., and Cole, G. J. (1995) Agrin is a heparan sulfate proteoglycan, *J. Biol. Chem.* **270,** 3392–3399.

Woodley, D. T., Rao, C. N., Hassell, J. R., Liotta, L. A., Martin, G. R., and Kleinman, H. K. (1983) Interactions of basement membrane components, *Biochim. Biophys. Acia* **761,** 278–283.

Yamada, Y., and Kuehn, K. (1993) Genes and regulation of basement membrane collagen and laminin synthesis, *in* D. H. Rohrbach and R. Timpl (Eds.), Molecular and Cellular Aspects of Basement Membranes, pp. 189–210. Academic Press, San Diego.

Yurchenco, P. D., and O'Rear, J. (1993) Supramolecular organization of basement membranes, *in* D. H. Rohrbach and R. Timpl (Eds.), Molecular and Cellular Aspects of Basement Membranes, pp. 19–47. Academic Press, San Diego, CA.

Yurchenco, P. D., and O'Rear, J. (1994) Basal lamina assembly, *Curr. Opin. Cell Biol.* **6,** 674–681.